Vacas, E. et al. (2014) 'Signalling pathways involved in antitumoral effects of VIP in human renal cell carcinoma A498 cells: VIP induction of p53 expression', The international journal of biochemistry & cell biology, 53, pp. 295–301.

Available at https://doi.org/10.1016/j.biocel.2014.05.036

Signalling pathways involved in antitumoral effects of VIP in human renal cell carcinoma A498 cells: VIP induction of p53 expression

Eva Vacas[a], Laura Muñoz-Moreno[a], Ana B. Fernández-Martínez[a], Ana M. Bajo[a], Manuel Sánchez-Chapado[b,c], Juan C. Prieto[a,*], María J. Carmena[a]

[a] *Department of Systems Biology, Unit of Biochemistry and Molecular Biology, University of Alcalá, 28871 Alcalá de Henares, Spain*

[b] *Department of Surgery and Medical and Social Sciences, Unit of Surgery, University of Alcalá, 28871 Alcalá de Henares, Spain*

[c] *Department of Urology, Príncipe de Asturias Hospital, 28871 Alcalá de Henares, Spain*

* Corresponding author. Juan C. Prieto, Department of Systems Biology, Unit of Biochemistry and Molecular Biology, University of Alcalá, 28871 Alcalá de Henares, Spain University of Alcalá, 28871 Alcalá´ de Henares, Spain, E-mail: juancarlos.prieto@uah.es; Tel.: +34 1 885 4527

Abstract

Vasoactive intestinal peptide (VIP) decreases cell proliferation through PI3K signalling and prevents tumour progression in clear renal cell carcinoma (RCC). Here we analyzed the signalling pathways that mediate such VIP effects by using human RCC A498 cells. The effects of treatment with 1 mM VIP and/or specific protein kinase inhibitors such as H89, Wortmannin and PD98059 were studied by cell adhesion assay, ELISA of VEGF165 and ROS production assays. Semiquantitative RT-PCR and western blot were performed to study p53 expression. VIP increased cell adhesion and ROS production, and decreased VEGF165 secretion through PI3K signalling. Moreover, VIP increased nuclear expression of tumour suppressor p53. VIP effects could be blocked by cell incubation with a specific p53 inhibitor, cyclin pifithrin-a hydrobromide (CPFT-αH). In conclusion, this study provides a p53-dependent mechanism by which VIP regulates cell proliferation in RCC development. It supports a potential usefulness of VIP in new therapies of RCC.

Keywords: VIP; PI3K; VEGF; p53; Renal cell carcinoma

1. Introduction

Renal cell carcinomas (RCCs) represent 3% of all adult cancers in Western populations (Dihazi, 2013). RCC is considered a clinicopathologically heterogeneous disease, clear cell carcinoma being the most common type of RCC since it accounts for 70% of all renal carcinomas (Gurel et al., 2013). Clear cell renal cell carcinomas (ccRCCs) are highly vascularized tumours, due to silencing of the tumour suppressor von Hippel-Lindau (VHL) gene or loss of chromosome 3p which leads to further production of proangiogenic growth factors such as vascular endothelial growth factor (VEGF) (Bienes-Martínez et al., 2012). This factor is, to date, the key element in the pathogenesis of RCC. VEGF pathway activation is responsible for the recruitment, migration, and expansion of endothelial cells, i.e. an angiogenesis tumour model characteristic of RCC (Albiges et al., 2011).

The genetic alterations responsible for oncogenesis and tumour progression may underline the ability of renal cell carcinomas to switch to an angiogenic phenotype. Activation of p53 is driven by a wide variety of stress signals that a cell might encounter during malignant progression (genotoxic damage, oncogene activation or loss of normal cell contacts) leading to a model in which the growth inhibitory functions of p53 are normally held dormant (Vousden and Lane, 2007). Functional inactivation of the p53 pathway is observed in most human tumours and results from mutations in the p53 gene itself (50% of cases) or reversible inhibition. So, in a half of human cancers, activation of p53 function is considered a promising anticancer strategy (Dey et al., 2008). Therefore, loss of p53 has been postulated to lead to more aggressive tumours. Interestingly, p53 mutations have been detected in 20–30% of primary and 70–80% of metastatic renal tumours, suggesting that mutations are associated with progression of RCC (Angelo et al., 2002). Also, p53 can exert several effects on tumour suppression including the inhibition of angiogenesis by

downregulating VEGF expression (Farhang et al., 2013) and the inhibition of tumour growth and metastasis (Brady and Attardi, 2010).

Vasoactive intestinal peptide (VIP) is a neuropeptide that acts mainly through VPAC1 and VPAC2 receptors (Laburthe et al., 2007) and mediates many physiological and pathophysiological processes, such as growth, cancer, immune responses, circadian rhythms, control of neuronal and endocrine cells, and functions of the digestive, respiratory, reproductive and cardiovascular systems (Vaudry and Laburthe, 2006). VIP receptors are members of the G-protein-coupled receptor (GPCR) superfamily and lead to adenylate cyclase (AC) activation, cAMP production, and PKA (protein kinase A) or EPAC (exchange protein activated by cAMP) pathway activation (Laburthe et al., 2007; Vaudry and Laburthe, 2006; Dickson and Finlayson, 2009) as well as to the stimulation of CREB (cAMP response element-binding protein) (Guan et al., 2009), PKC (protein kinase C) (Dickson and Finlayson, 2009), PI3K (phosphatidylinositol 3-kinase) (Herrera et al., 2009; Zhang et al., 2010) and several cellular transcription factors such as CRE, NFKB (nuclear factor KB) and AP-1 (activator protein-1) (Delgado and Ganea, 2000; Moody and Gozes, 2007).

In RCC, we have shown that VIP inhibits cell proliferation in A498 cells through VPAC1/AC/cAMP/PI3K pathway (Vacas et al., 2012). Moreover, the efficacy of VIP on the prevention of RCC progression was confirmed in vivo using xenografted athymic mice (Vacas et al., 2013). Also, we have observed the involvement of VIP in several steps of the metastatic phenotype development in RCC. VIP, acting through VPAC1/2 receptors, prevents cell invasion and migration, increases cell adhesion, reduces VEGF levels and is able to increase ROS (reactive oxygen species) production in A498 cells, managing a non-favourable environment in renal cell carcinoma (Vacas et al., 2013). In this context, the

aims of the present study were to investigate the signalling pathways involved in these VIP effects and the possible role of p53 in all them. The characterization of protein-expression alterations in RCC, especially metastasizing RCC, may provide insight into important changes in the corresponding functional pathways, thus allowing a better knowledge of the fundamental mechanisms of RCC development and progression at the molecular level. It is interesting to note that VIP presents important structural and functional homologies with pituitary adenylate cyclase activating peptide (PACAP). In fact, both peptides show similar affinity for VPAC1 and VPAC2 receptors whereas PACAP also recognizes PAC1 receptor with high affinity (Laburthe et al., 2007; Vaudry and Laburthe, 2006). Much work has been made on cyto- protective effects of PACAP in the kidney against different harmful situations (revised in Reglodi et al., 2012). In particular, protective action of PACAP38 on models of kidney injury appears to involve VPAC1 and PAC1 receptors but not VPAC2 receptors (Arimura et al., 2006). The broad knowledge on PACAP role in this organ led us to advance in the scarcely studied relevancy of VIP at this level. Present results contribute to suggest that not only PACAP but also VIP are emerging candidates for treatment of human kidney pathologies.

2. Materials and methods

2.1. Cell culture

The human renal cell carcinoma cell line A498 (VHL null) was purchased from the American Type Culture Collection (ATCC, Rockwell, MD, USA). Cell culture was carried out in Eagle's Modified Medium (ATCC) supplemented with 10% foetal bovine serum, 1% penicillin/streptomycin/amphotericin B. The culture was performed in a humidified 5% CO_2 environment, at 37 °C. After cells reached 70–80% confluence, they were washed

with PBS, detached with 0.25% trypsin/0.2% EDTA, and plated at 30,000–40,000 cells/cm^2. The culture medium was changed every 2 days. Cells were serum-deprived for 24 h and then treated with 1 μM VIP for different times in the absence of serum.

2.2. Reagents

VIP was purchased from Neo MPS (Strasbourg, France). Cyclin pifithrin-a hydrobromide (CPFT-αH) from Telstar (Dewsbury, UK), PD98059 from Alexis (San Diego, CA, USA), forskolin and H89 from Sigma–Aldrich (Alcobendas, Madrid, Spain), and 2›,7›- dichlorodihydrofluorescein diacetate (H_2DCFDA) from Molecular Probes (Life Technologies). Antibodies directed against p53 and í3-actin were purchased from Sigma–Aldrich.

2.3. Cell adhesion assay

A concentrated stock of type-I collagen solution was diluted in 10 nM glacial acetic acid and coated into 96-well plates for 1 h at 37 °C. Then, plates were washed twice with PBS (pH 7.4). On the other hand, A498 cells were harvested with 0.25% trypsin/0.2% EDTA and collected by centrifugation. Pelleted cells were resus- pended in serum-free medium with 0.1% (w/v) BSA (pH 7.4), plated at 25 × 10^3 cells/100 μl, and treated with VIP or forskolin for 30 min. Moreover, they were preincubated with one of three different protein kinase inhibitors: PKA inhibitor H89 (15 min), MEK1/2 inhibitor PD98059 (1 h) or PI3K inhibitor Wortmannin (30 min), and then with 1 μM VIP for 30 min. The assay was finished by aspi- ration of the wells. Cell adhesion was quantified by adding 1 mg/ml solution of 3-(4,5-dimethylthiazol-2-yl)-2,5-diphenyl tetrazolium bromide (MTT) (Sigma–Aldrich) for reduction into a blue formazan dye by

viable mitochondria. Afterwards, the medium was discarded and 100 µl isopropanol was added to dissolve the blue-coloured formazan particles, and absorbance was reported at 680 nm with a reference wavelength at 720 nm.

2.4. ROS levels

A498 cells (15×10^4 cells per well) in 6-well plates were treated with VIP or forskolin for 24 h. Moreover, they were preincubated with one of three different protein kinase inhibitors: PKA inhibitor H89 (15 min), MEK1/2 inhibitor PD98059 (1 h) or PI3K inhibitor Wortmannin (24 h), and then with 1 µM VIP for 24 h. Afterwards, the cells were washed with PBS and then detached with 0.25% trypsin/0.2% EDTA. The cells were centrifuged at 1200 rpm for 5 min at 4 °C and the pellets were mixed with CM-H_2DCFDA (chlorometil-2›,7›-dichlorofluorescein) staining (ROS Detection Reagents, Molecular Probes, Invitrogen) for 1 h at 37 °C. Then, the tubes were centrifuged, the supernatants removed and the pellets resuspended in 1× PBS, 0.2 mg/ml RNase A and 20 µg/ml propidium iodide (PI) before flow cytometric analysis.

2.5. Measurement of catalase activity

A498 cells (15×10^4 cells per well) in 6-well plates were treated with 1 µM VIP for 2 h. The cells were washed twice with ice-cold PBS and then harvested, scraped into ice-cold PBS, and pelleted by centrifugation at 500 × *g* for 5 min at 4 °C. Cytosolic proteins were isolated as described in Section 2.8. Then, 100 µl cytosolic extract was mixed with 900 µl PBS and next with 1 ml hydrogen peroxide; finally, absorbance was measured at 240 nm for 5 min.

2.6. Measurement of VEFG$_{165}$ levels

A498 cells were placed in 24-well plates (75×10^3 cells per well) and maintained in their medium for 24 h. Cells were treated with VIP and forskolin for 24 h. Moreover, they were preincubated with one of three different protein kinase inhibitors: PKA inhibitor H89 (15 min), MEK1/2 inhibitor PD98059 (1 h) or PI3K inhibitor Wortmannin (30 min), and then with 1 μM VIP for 24 h. Thereafter, the medium was removed and kept at −80 °C for ELISA. VEGF$_{165}$ was analyzed using a human VEGF DuoSet kit (R&D Systems, Minneapolis, MN, USA).

2.7. RNA isolation and RT-PCR

A498 cells were placed in 6-well plates (15×10^3 cells) and incubated with 1 μM VIP in serum medium for different periods of time. Total RNA was isolated with Tri-Reagent (Sigma) according to the instructions of the manufacturer. Two μg of total RNA were reverse-transcribed using 6 μg of hexamer random primer and 200 U M-MLV RT (Life Technologies) in the buffer supplied with the enzyme, supplemented with 1.6 μg/ml oligo dT, 10 nM dithiothreitol (DTT), 40 U RNasin (Promega Madison, WI, USA), and 0.5 mM deoxyribonucleotides (dNTPs). Two μl of the RT reaction were used for each PCR amplification with a primer set which amplifies cDNAs for human cysteine rich protein with p53 or í3-actin. The corresponding sequences of oligonucleotide primers were: p53 (sense 5›-AGG CCT TGG AAC TCA AGG AT-3› and antisense 5›-TGA GTC AGG CCT TCT GTC T-3›); p21/WAF1 (sense 5›-ATG AAA TTC ACC CCC TTT CC-3› and antisense 5›-AGG TGA GGG GAC TCC AAA GT-3›); and í3-actin (sense 5›-AGA AGG ATT CCT ATG TGG GCG-3› and antisense 5›-CAT GTC GTC CCA GTT GGT

GAC-3›). PCR-conditions were: denaturation at 94 °C for 5 min, followed by 26–40 cycles of 95 °C for 1 min, 57 °C for 1 min, 72 °C for 1 min, and then a final cycle of 10 min at 72 °C. The signals were normalized with the í3-actin gene expression level. The PCR products were separated by electrophoresis and visualized in 2% agarose gels. The bands were cut from the gel, eluted, and automatically sequenced with an ABI 377 sequencer (Applied Biosystems, Alcobendas, Madrid, Spain).

2.8. Cytosolic and nuclear protein isolation and western blotting

A498 cells in 100 mm cell culture dishes ($1–2 \times 10^6$ cells) were incubated with 1 μM VIP for different time periods. The cells were washed twice with ice-cold PBS and then harvested, scraped into ice-cold PBS, and pelleted by centrifugation at $500 \times g$ for 5 min at 4 °C. Cytosolic and nuclear contents were extracted with a commercially available kit according to manufacturer's instruction (NE-PER®, Nuclear and Cytoplasmic Extraction Reagents) (Thermo Scientific, Rockford, IL, USA). Protein content was measured by the Bradford assay using BSA as a standard. Cytosolic protein was booked to analyze catalase activity (2.5). Nuclear protein (15 μg) was solubilized in 50 mM Tris–HCl buffer (pH 6.8) containing 10% (v/v) glycerol, 3% (w/v) SDS, 0.01% bromophenol blue, and 0.7 M β-mercaptoethanol, and then heated at 95 °C for 5 min. Nuclear proteins were resolved by 10% SDS- PAGE, and transferred to nitrocellulose sheets (BioTrace/NT, Pall Corporation, East Hills, NY, USA). Mouse monoclonal anti-p53 (Sigma–Aldrich) (1:2000) antibody was added followed for overnight incubation. After treatment for 1 h at room temperature with the corresponding HRP-labelled secondary antiserum (BD Biosciences) (1:4000), the signals were detected with

enhanced chemiluminescence reagent (Amersham, Uppsala, Sweden) using í3-actin antibody (Sigma–Aldrich) (1:10,000) for loading control.

2.9. Cell proliferation assay with 5′-bromo-2′deoxyuridine (BrdU)

A498 cells were plated in 6-well plates (15×10^4 cells per well) and maintained in medium for 24 h. The cells were treated with 1 μM VIP for 24 h and pulsed with 40 μM BrdU (BD Bioscience) in the last hour of incubation. Afterwards, the cells were washed with PBS and fixed with ice-cold absolute ethanol, at −20 °C, for 30 min. Fixative was removed by centrifugation and the cell pellets were washed with PBS. DNA was partially denatured by incubation with 2 M HCl for 30 min at room temperature. Thereafter which the cells were washed three times with PBS containing 0.05% Tween-20 (pH 7.4) and 0.1% BSA. Cells were incubated for 1 h with 20 μl of anti-BrdU monoclonal antibody with FITC (BD Bioscience) in the dark. The cells were stained with PI staining solution (50 μg/ml PI, 10 μg/ml RNase, 1× PBS) and subjected to flow cytometric analysis. The amount of DNA distribution in the difference phases of the cell cycle was analyzed with the use of the Cyflogic v. 1.2.1 program (CyFlo Ltd., Turku, Finland).

2.10. Data analysis

Quantification of band densities was performed using the Quantified One Program (Bio-Rad). Data shown in the figures are representative of at least three independent experiments. The results are expressed as the mean ± SEM and were statistically treated following the Bonferroni's test for multiple comparisons after one or two-way analysis of variance (ANOVA). The level of significance was set at $P < 0.05$.

3. Results

3.1. Signal transduction pathways involved in VIP effect on cell adhesion

To explore the pathways involved in VIP effect on A498 cell adhesion, cells were suspended and incubated for 30 min with 1 μM VIP or 0.1 μM forskolin. Then, cells were placed in 96-well plates with collagen for 40 min (Fig. 1). Thereafter, the cells were incubated with MTT and measured by cell adhesion assay. The involvement of the cAMP pathway was confirmed by the observation of the stimulatory effect of 0.1 μM forskolin upon cell adhesion.

To evaluate the specificity of the signalling pathways that could be involved in VIP effect on cell adhesion in renal carcinoma cells, A498 cells were cultured in the absence or presence of 1 μM VIP and different protein kinase inhibitors: PKA inhibitor H89, MEK1/2 inhibitor PD98059, or PI3K inhibitor Wortmannin. As shown in Fig. 1, cell treatment with 0.1 μM Wortmannin fully abolished the stimulatory effect of VIP upon the adherent capacity of A498 cells, whereas 10 μM H89 and 10 μM PD98059 had no effect. These results support that PI3K plays a role in the effect of VIP on cell adhesion in A498 cells.

3.2. Signal transduction pathways involved in VIP effect on $VEGF_{165}$ secretion

To know the signalling pathways involved in the angiogenic effect of VIP, secretion levels of VEGF were measured in A498 cells treated with forskolin and inhibitors of protein kinases and/or VIP at 4 h by ELISA. The results shown in Fig. 2 indicate that both forskolin and VIP decreased VEGF levels in a similar manner. Furthermore, pretreatment with various protein kinase inhibitors and subsequent incubation with VIP showed that Wortmannin blocked the effect of the neuropeptide on $VEGF_{165}$ secretion levels. Thus,

the PI3K pathway appears to be directly involved in the antiangiogenic effect of VIP.

3.3. Signal transduction pathways involved in VIP effect on intracellular ROS levels

We evaluated the involvement of the second messenger cAMP and analyzed the effect of protein kinase inhibitors in the production of ROS in A498 cells by means of a CM-H_2DCFDA incorporation assay. A498 cells were incubated for 2 h with a direct AC stimulator, forskolin. As shown in Fig. 3, forskolin produced a significant increase, similarly to VIP, of ROS levels. On the other hand, treatment with protein kinase inhibitors suggests that VIP increases ROS levels in renal tumour cells through two signalling pathways. Both Wortmannin and PD98059 completely reversed the effect of VIP on ROS levels (Fig. 3), which involves PI3K and MEK1/2 as mediators of increased radical levels in A498 cells.

3.4. Effect of VIP on p53 expression

The effect of VIP on A498 cell proliferation was determined in a previous work by our research group (Vacas et al., 2012), showing that VIP is able to reduce the proliferative capacity of A498 cells. In an attempt to know the cause of the decreased number of cells, we proposed to assess p53 expression levels. Cells were treated with 1 μM VIP at various times and analyzed by semiquantitative RT-PCR and western blot; í3-actin was used as load control. Fig. 4A shows that VIP, after 15 min incubation, significantly increased the expression levels of p53 mRNA in A498 cells (up to 50%), maintaining this effect at all times studied. Moreover, we analyzed the expression levels of p21/WAF1 mRNA, one of the effectors of p53, which is important in the DNA-damage checkpoint. Fig. 4B shows that VIP also significantly increased them. It is related with previous results from our laboratory showing a decrease of PCNA levels in A498 cells treated with VIP (Vacas et al., 2012), which is probably due to this increase of p21 expression upon treatment with

the neuropeptide. Further analysis of p53 expression by western blot revealed that VIP treatment produced a significant increase of p53 protein levels in tumour cells (Fig. 4C). This increase of p53 could explain the decrease observed in A498 cell proliferation.

Moreover, we decided to evaluate whether VIP-increased p53 expression is mediated by cAMP and PI3K signalling. We treated A498 cells with 0.1 μM forskolin or 0.1 μM Wortmannin and then a western blot was carried out. Forskolin increased p53 expression, relating directly cAMP in VIP effect on p53 expression. The involvement of PI3K was confirmed by the observation of the inhibitory effect of Wortmannin upon VIP-stimulated p53 expression (Fig. 4D).

3.5. Involvement of p53 in VIP effects on cell proliferation, cell adhesion, ROS production, catalase activity and $VEGF_{165}$ secretion

Once observed that VIP-decreasing proliferation of A498 cells could be related to an increase of p53 expression, we proposed to treat tumour cells with the p53 inhibitor CPFT-αH. This procedure served to analyze the role of p53 in the decrease of cell proliferation and secretion levels of $VEGF_{165}$, and the increase of cell adhesion and intracellular levels of ROS that VIP elicits in A498 cells. Fig. 5 shows that CPFT-αH blocks VIP effect on inhibition of cell proliferation (Fig. 5A), increase of both cell adhesion (Fig. 5B) and ROS production (Fig. 5C), and decrease of catalase activity (Fig. 5D) and VEGF secretion (Fig. 5E) in A498 tumour cells. These results support p53 involvement in antiproliferative effects of VIP in RCC.

4. Discussion

The present study reveals that VIP induces p53 expression at both mRNA and protein levels in the human renal cell carcinoma A498 cell line (VHL null). This oncosuppressor

role of VIP appears to be mediated by stimulation of cAMP production and involvement of PI3K signalling pathway leading to increase of cell adhesion and intracellular ROS levels, and decrease of cell proliferation and VEGF secretion. Previous results from our laboratory with this cell line showed the inhibitory effect of VIP effect on cell proliferation and hence on the growth of tumour mass (Vacas et al., 2012). In the same study, we observed the VIP ability in reducing metastatic progression and increasing ROS levels in A498 cells. Also, we determined VEGF secretion in this human VHL-null tumour cell line showing that VIP decreased the high secretion levels of VEGF that provokes this genetic disruption. In this context, we decided to carry out experiments in order to know the signalling pathways involved in these tumoral processes. It is interesting to note that we have previously measured the endogenous expression of VIP in tumour A498 and normal HK2 cells. Both human kidney cell lines exhibited basal levels of mRNA as well as of cytosolic and secreted VIP. Comparison of basal levels showed a significant increase of endogenous VIP production in tumour A498 cells versus non-tumour HK2 cells (Vacas et al., 2012).

The PI3K pathway has an important role in modulating cell growth, proliferation, metabolism, survival and angiogenesis (Sheppard et al., 2012). Activation of the PI3K pathway in many cancer types has been demonstrated in numerous studies. The most common mutations are that of p110a (PI3KCA) and loss of the tumour suppressor PTEN. There is specific evidence of PI3K path- way activation in RCC; it is constitutively activated in RCC cells regardless of VHL status, and activation is tumour specific (Elfiky et al., 2011).

Epithelial cells undergo changes in morphology and binding capacity during the transformation to an invasive carcinoma. Thus, they lose polarity and differentiate into a

phenotype with increased motility and invasiveness (Reuter et al., 2010). In this work, we studied the signalling pathways involved in the effect of VIP on cellular adhesion. Results showed increased levels of cAMP and activation of the PI3K pathway, and indicated that VIP induced tumour cells to adhere to the matrix, decreasing the number of cells with the capacity of invasion. Several studies have reported that the loss of VHL in clear cell RCC can induce cellular invasive- ness, causing the loss of E-cadherin, facilitating the separation of the epithelial cells, and allowing cell migration (Vacas et al., 2013; Evans et al., 2007; Lineham et al., 2007). Thus, treatment with VIP may induce a change from a migratory phenotype, typical of tumour cells, to a stationary phenotype, typically found in normal epithelial cells.

Angiogenesis is a process essential for tumour growth and metastasis in which the VEGF signalling pathway plays a main role. In particular, VEGF-mediated signalling is considered important for CCR, due to deregulation by loss of VHL protein (Bhargava and Robinson, 2011). Here we assessed the effect of VIP on the secretion of $VEGF_{165}$ isoform by AC/cAMP/PI3K. VIP treatment of A498 cells reduced their high levels of VEGF secretion into the extracellular medium. This is a promising result, since most clinical trials for RCC are based on VEGF inhibition (Wright and Kapoor, 2011; Cáceres and Cruz-Chacón, 2011; Pirrotta et al., 2011; Posadas and Figlin, 2012). VIP appears to exert antiangiogenic effects through increased expression of p53, as observed in this study. The signalling events acting in the antiangiogenic effect of VIP are associated with an increase of cAMP, which would be involved in the PI3K pathway.

VIP-dependent decrease of A498 cell proliferation is conceiv- ably caused by increased p53 expression as shown with CPFTa-H treatment. It may be related to a previous increase of intracellular ROS levels and decrease of catalase activity, by

possible activation of cellular mechanisms of defence. The relationship between cell proliferation and ROS levels is suggested by the observation of the same PKA-independent cAMP/PI3K signalling pathway for VIP stimulation of intracellular ROS levels and reduction of cell proliferation in A498 cells. It has been reported that high concentrations of ROS can cause the activation and stabilization of p53 and, thus, the reactivation of p53 in tumours from mice lacking sup- pressor protein causes complete tumour regression (Trachootham et al., 2008). Similar effects were observed with anti-tumour agents based on increasing ROS and stimulation of p53, whereas a high sensitivity to pro-oxidants have been described in RCC (Gupta et al., 2012; Sourbier et al., 2010). Moreover, STAT3 acts as a repressor of p53 expression and exerts a collaboration and crosstalk with NFKB in inhibition of apoptosis (Grivennikov et al., 2010). Thus, activation of and interaction between STAT3 and NFKB plays a key role in controlling the dialogue between the malignant cell and its microenvironment. In this way, the effect of VIP on the decrease of activation of these transcription factors, previously observed by our group (Vacas et al., 2012, 2013), together with increased intracellular ROS levels, result in stimulation of p53 expression that could be responsible for the decrease of the tumour cell proliferation. Although future research is needed to complete clarification of this point, our data suggest that this could be the mechanism by which VIP triggers antitumoral effects in A498 cells.

Conflict of interest statement

None declared

Acknowledgements

This work was supported by the Ministerio de Ciencia e Innovación (Grant SAF2007-

63794), Junta de Comunidades de Castilla la Mancha (Grant PII 1/09-0061-3802), Fundación Mutua Madrileña (Grant 2010-002), and Fundación Jesús Serra (Grupo Catalana de Occidente).

References

Albiges L, Salem M, Rini B, Escudier B. Hematol Oncol Clin North Am 2011;25:813–33.

Angelo LS, Talpaz M, Kurzrock R. Cancer Res 2002;62:932–40. Arimura A, Li M, Batuman V. Blood 2006;107:661–8.

Bhargava P, Robinson MO. Curr Oncol Rep 2011;13:103–11.

Bienes-Martínez R, Ordóñez A, Feijoo-Cuaresma M, Corral-Escariz M, Mateo G, Sten- ina O, et al. Sci Rep 2012;2:788.

Brady CA, Attardi LD. J Cell Sci 2010;123:2527–32. Cáceres W, Cruz-Chacón A. P R Health Sci J 2011;30:73–7. Delgado M, Ganea D. J Neuroimmunol 2000;110:97–105.

Dey A, Tergaonkar V, Lane DP. Nat Rev Drug Discov 2008;7:1031–40. Dickson L, Finlayson K. Pharmacol Ther 2009;121:294–316.

Dihazi H. Expert Rev Proteomics 2013;10:21–4.

Elfiky AA, Aziz SA, Conrad PJ, Siddiqui S, Hackl W, Maira M, et al. J Transl Med 2011;9:133.

Evans AJ, Russell RC, Roche O, Burry TN, Fish JE, Chow VWK, et al. Mol Cell Biol 2007;27:157–69.

Farhang GM, Goossens S, Nittner D, Bisteau X, Bartunkova S, Zwolinska A, et al. Cell Death Differ 2013;10:1038.

Grivennikov SI, Karin M, Cytokine. Growth Factor Rev 2010;21:11–9.

Guan CX, Cui YR, Sun GY, Yu F, Tang CY, Li YC, et al. Regul Pept 2009;153: 64–9.

Gupta SC, Hevia D, Patchva S, Park B, Koh WW, Aggarwal BB. Antioxid Redox Signal 2012;16:1295–322.

Gurel S, Narra V, Elsayes KM, Siegel CL, Chen ZE, Brown JJ. Diagn Interv Radiol 2013;19:304–11.

Herrera JL, Gonzalez-Rey E, Fernandez-Montesinos R, Quintana FJ, Najmanovich R, Pozo D. J Cell Mol Med 2009;13:3209–17.

Laburthe M, Couvineau A, Tan V. Peptides 2007;28:1631–9.

Lineham WM, Pinto PA, Srinivasan R R, Merino M, Choyke P, Choyke L, et al. Clin Cancer Res 2007;13:671–9.

Moody TW, Gozes I. Curr Pharm Des 2007;13:1099–104.

Pirrotta MT, Bernardeschi P, Fiorentini G. Curr Med Chem 2011;18:1651–7. Posadas EM, Figlin RA. Oncology 2012;26:290–301.

Reglodi D, Kiss P, Horvath G, Lubics A, Laszlo E, Tamas A, et al. Neuropeptides 2012;46:61–70.

Reuter S, Gupta SC, Chaturvedi MM, Aggarwal BB. Free Radic Biol Med 2010;49:1603–16.

Sheppard K, Kinross KM, Solomon B, Pearson RB, Phillips WA. Crit Rev Oncog 2012;17:69–95.

Sourbier C, Valera-Romero V, Giubellino A, Yang Y, Sudarshan S, Neckers L, et al. Cell Cycle 2010;9:4183–9.

Trachootham D, Lu W, Ogasawara MA, Rivera-del Valle N, Huang P. Antioxid Redox

Signal 2008;10:1343–74.

Vacas E, Fernández-Martínez AB, Bajo AB, Sánchez-Chapado M, Schally AV, Prieto JC, et al. Biochim Biophys Acta: Mol Cell Res 2012;1823:1676–85.

Vacas E, Bajo AM, Schally AV, Sánchez-Chapado M, Prieto JC, Carmena MJ. Mol Cell Endocrinol 2013;365:212–22.

Vaudry H, Laburthe M. Ann NY Acad Sci 2006;1070:1–633. Vousden KH, Lane DP. Nat Rev Mol Cell Biol 2007;8:275–83. Wright I, Kapoor A. Curr Opin Support Palliat Care 2011;5:211–21.

Zhang S, Liu Y, Guo S, Zhang J, Chu X, Jiang C, et al. J Physiol Sci 2010;60: 389–97.

Figure legends

Fig. 1. Effect of protein kinase inhibitors on VIP decrease of cell adhesion in A498 cells. Cells were preincubated with H89 (15 min), Wortmannin (30 min) or PD98059 (1 h). Then, cells were incubated in suspension with VIP or forskolin (30 min). Finally, they were placed for 40 min, on a plate p-96 pretreated with type-I collagen. Measurement of cell adhesion was performed by colorimetric assays (> = 570/630 nm). Results are representative of at least three independent experiments and they are the mean ± SEM, $*P < 0.05$, $***P < 0.001$, compared with untreated control, and $^{###}P < 0.001$, compared with cells treated with VIP.

Fig. 2. Effect of different protein kinase inhibitors on the effect of VIP on VEGF165 secretion in A498 cells. Cells were preincubated with H89 (15 min), Wortmannin (30 min) and PD98059 (1 h). Then, cells were incubated with VIP or forskolin (4 h). Finally, supernatant was collected for ELISA measurement of VEGF165. Results correspond to the mean ± SEM and are representative of at least three independent experiments, $***P < 0.001$, versus control, and $^{##}P < 0.01$, compared with cells treated with VIP.

Fig. 3. Effect of protein kinase inhibitors on VIP increase of ROS levels in A498 cells. Cells were preincubated with H89 (15 min), Wortmannin (30 min) or PD98059 (1 h). Thereafter, cells were incubated for 2 h with VIP or forskolin. Then, cells were treated for 1 h with CM-H2 DCFDA. The cells were subjected to flow cytometric analysis. Results are the average of fluorescence per cell and are

shown as percentage of fluorescence with respect to the untreated control. Data are the mean ± SEM, ***$P < 0.001$, compared to untreated control, and ### $P <$ 0.001, compared to cells treated with VIP. All results are representative of at least three independent experiments.

Fig. 4. Time-dependent effect of VIP on p53 expression in A498 cells as measured by RT-PCR (A) and Western blot (B). Involvement of cAMP and PI3K in p53 protein expression (C). In Wortmannin treatment, cells were preincubated with the inhibitor for 30 min. Cells were incubated for 2 h with VIP or forskolin. The results are normalized to í3-actin and represent the mean values of three experiments ± SEM, *$P < 0.05$, **$P < 0.01$, ***$P < 0.001$ versus untreated cells, and ## $P < 0.01$, compared to cells treated with VIP.

Fig. 5. Involvement of p53 on VIP effects on cell proliferation (A), cell adhesion (B), ROS production (C), catalase activity (D), and $VEGF_{165}$ secretion (E) in A498 cells. Cells were incubated for 2 h with the specific p53 inhibitor (CPFT-αH). The results are the mean ± SEM of three experiments. *$P < 0.05$, **$P <$ 0.01, ***$P < 0.001$ compared with control without VIP.

Figure 1

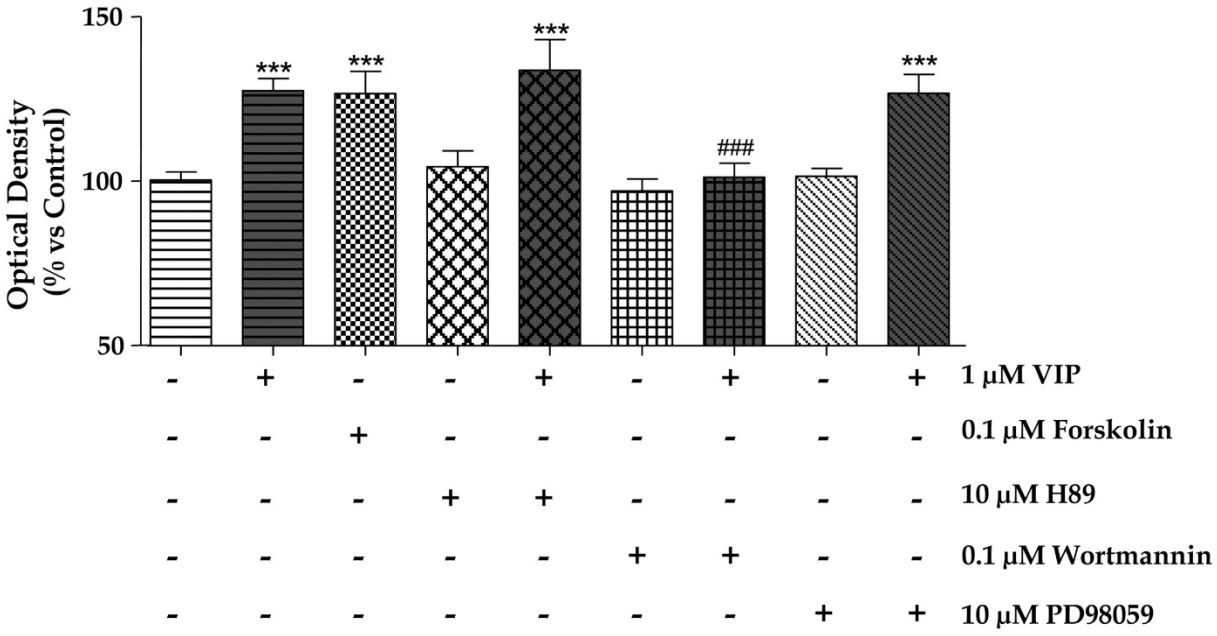
Optical Density
(% vs Control)
150
100
50
***
***
***
###
***
- + - - + - + - + 1 μM VIP
- - + - - - - - - 0.1 μM Forskolin
- - - + + - - - - 10 μM H89
- - - - - + + - - 0.1 μM Wortmannin
- - - - - - - + + 10 μM PD98059

Figure 2

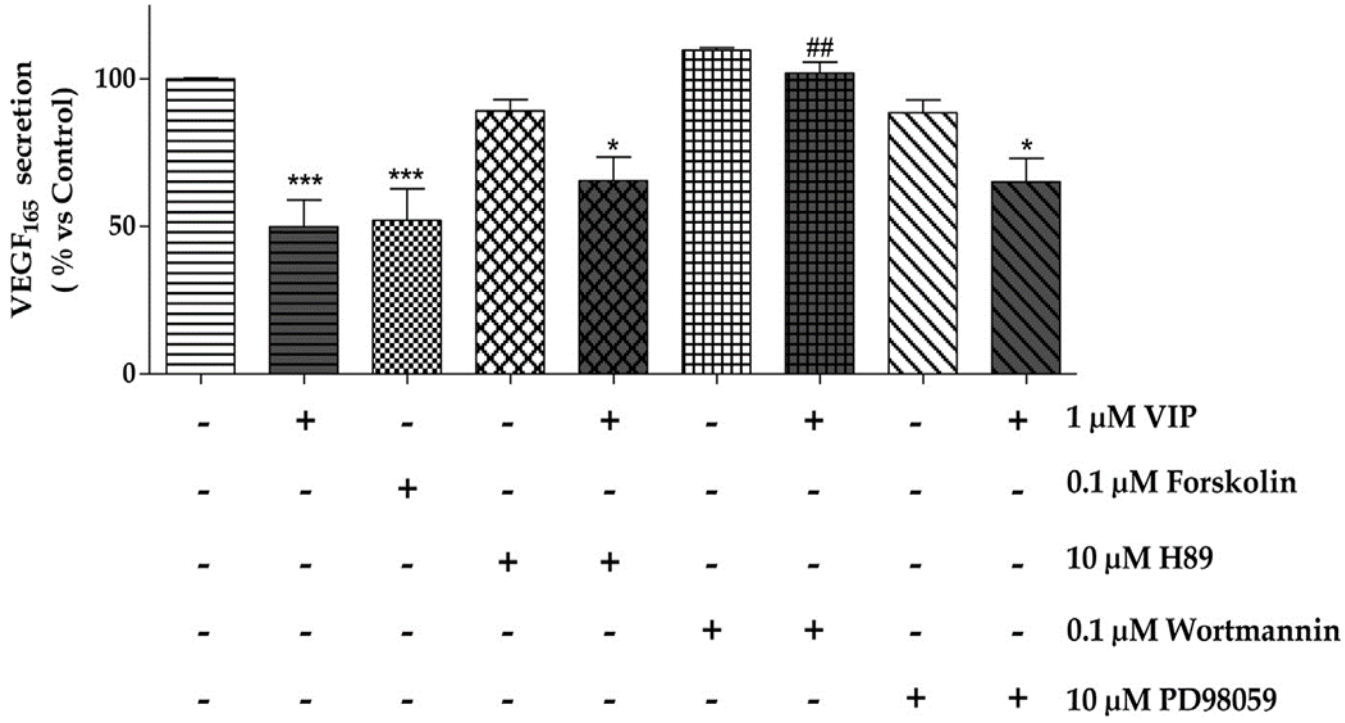
VEGF165 secretion
(% vs Control)
100
50
0
***
***
*
##
*
- + - - + - + - + 1 μM VIP
- - + - - - - - - 0.1 μM Forskolin
- - - + + - - - - 10 μM H89
- - - - - + + - - 0.1 μM Wortmannin
- - - - - - - + + 10 μM PD98059

Figure 3

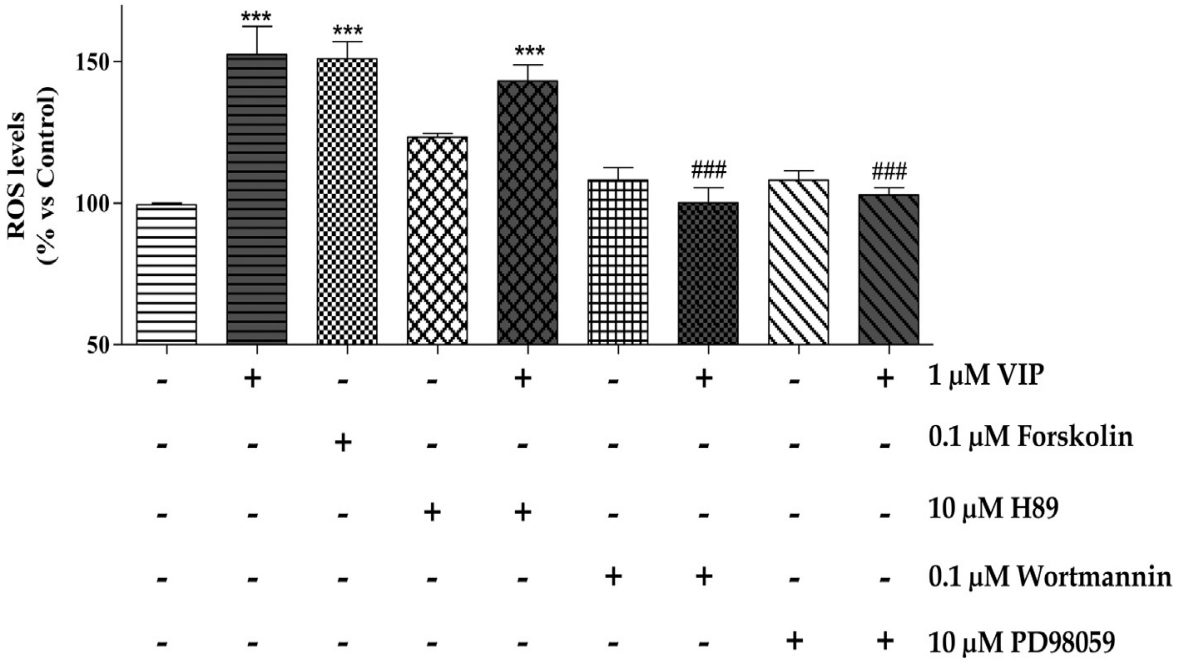
ROS levels
(% vs Control)
150
100
50
***
***
***
###
###
- + - - + - + - + 1 μM VIP
- - + - - - - - - 0.1 μM Forskolin
- - - + + - - - - 10 μM H89
- - - - - + + - - 0.1 μM Wortmannin
- - - - - - - + + 10 μM PD98059

Figure 4

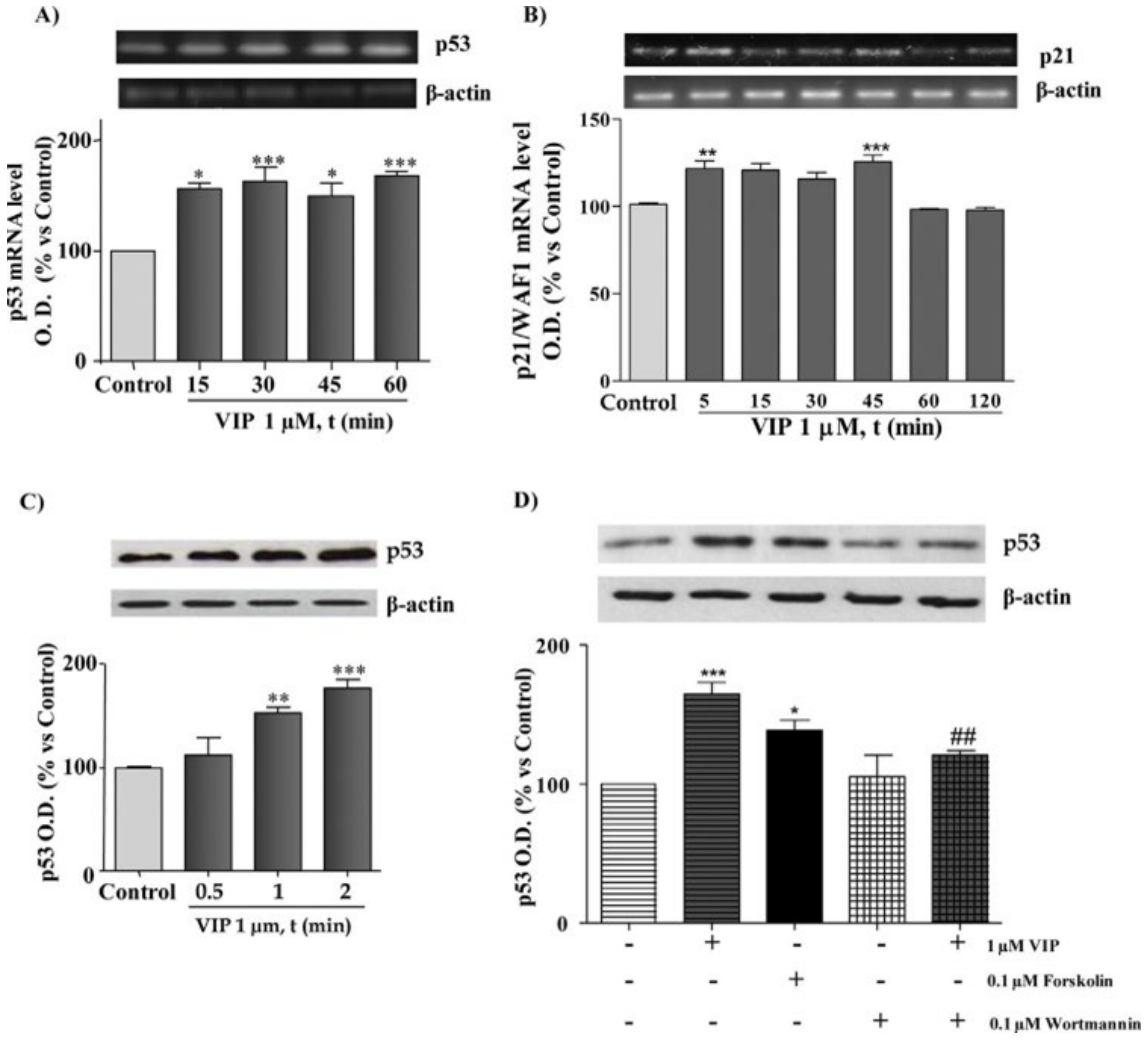
A)
p53
β-actin
p53 mRNA level
O. D. (% vs Control)
200
100
0
Control
15
30
45
60
VIP 1 μM, t (min)
B)
p21
β-actin
p21/WAF1 mRNA level
O.D. (% vs Control)
150
100
50
0
Control
5
15
30
45
60
120
VIP 1 μM, t (min)
C)
p53
β-actin
p53 O.D. (% vs Control)
200
100
0
Control
0.5
1
2
VIP 1 μm, t (min)
D)
p53
β-actin
p53 O.D. (% vs Control)
200
100
0
1 μM VIP
0.1 μM Forskolin
0.1 μM Wortmannin

Figure 5

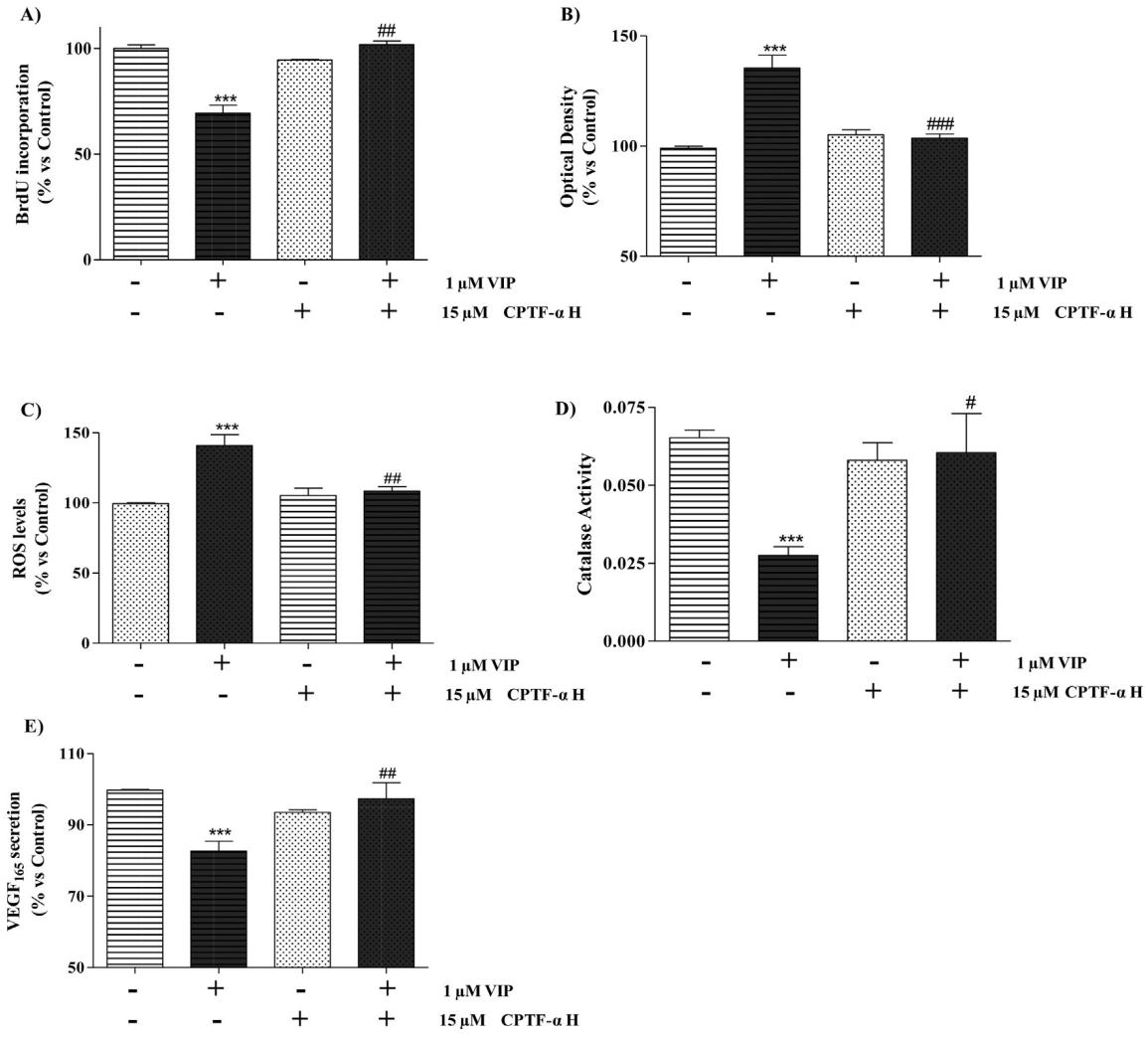
A)
BrdU incorporation (% vs Control)
100
50
0
***
##
B)
Optical Density (% vs Control)
150
100
50
***
###
1 µM VIP
15 µM CPTF-α H
C)
ROS levels (% vs Control)
150
100
50
0
***
##
D)
Catalase Activity
0.075
0.050
0.025
0.000
***
#
E)
VEGF165 secretion (% vs Control)
110
90
70
50
***
##

Supplementary data

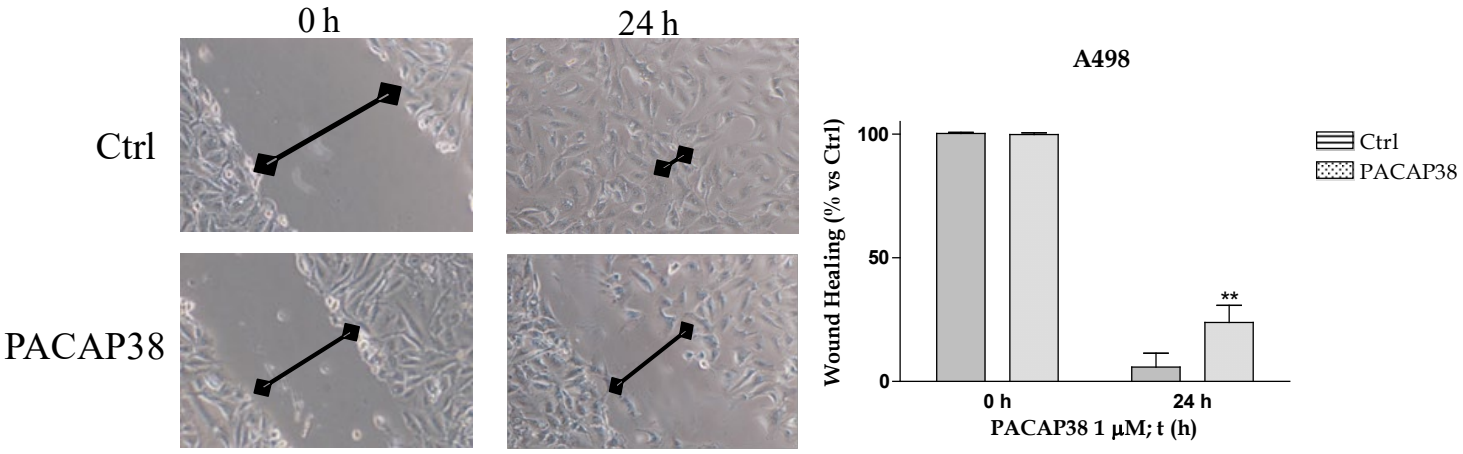

Annexe 1. We performed cell migration assays upon treatment for 24 h with PACAP38. This VIP-related peptide decreased the migratory activity as compared to the untreated control. The effect of PACAP38 was similar to that shown by VIP treatment in the same cell line (see Fig. 4 in Vacas et al., 2013).

Wound-healing assay followed this protocol: A498 cells were incubated in 24-well plates and a small wound area was made in the confluent monolayer with a scrapper. Afterwards, cells were incubated in the absence or presence of PACAP38 (1 µM). Three representative fields of each wound were captured using a Nikon Diaphot 300 inverted microscopy at 0 and 24 h. Wound areas of untreated samples were averaged and assigned a value of 100%.

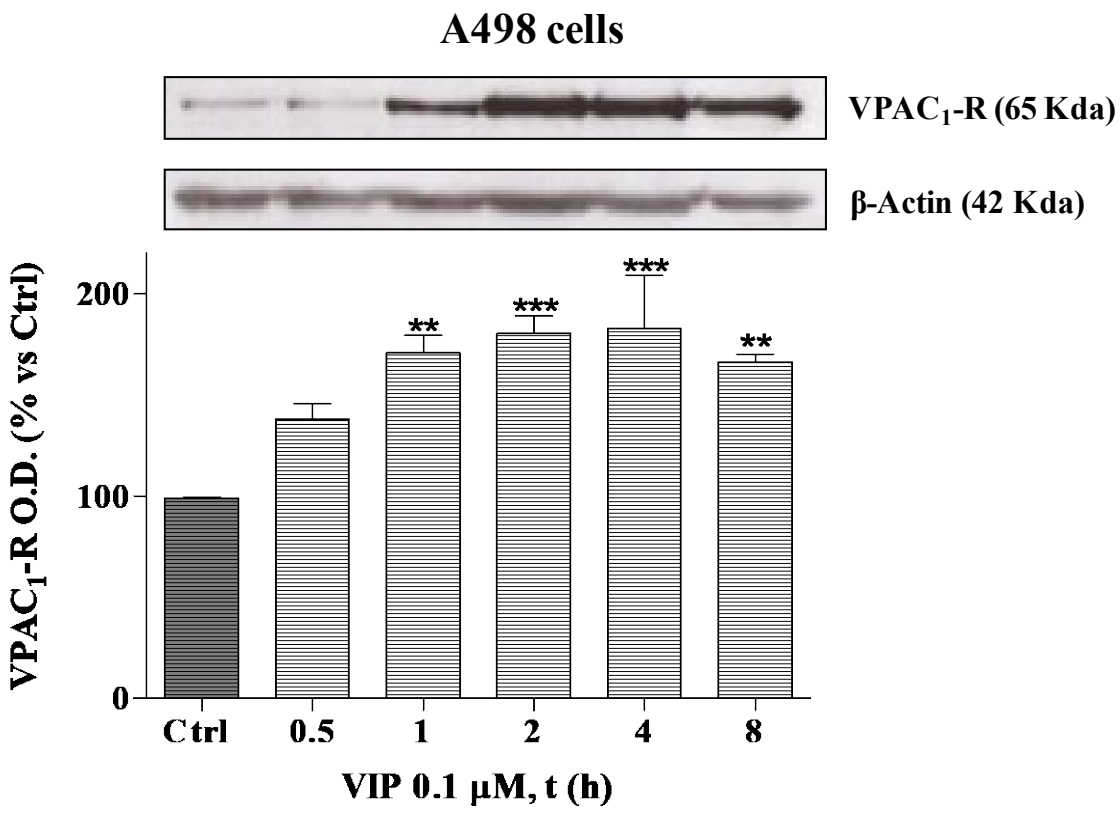

Annexe 2. The expression of VIP and its receptors in A498 cells has been previously studied by our group (Vacas et al., 2012). That report also shows the effect of VIP on its own expression and secretion. Here, we have also studied the effect of VIP on the expression of the majoritary VPAC1 receptor.

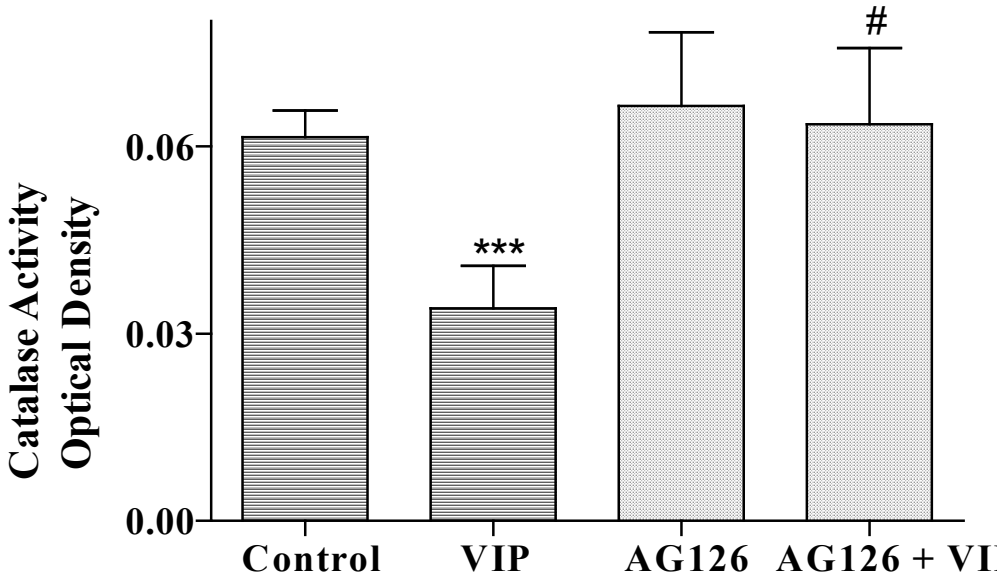

Annexe 3. Involvement of MAPK cascade in VIP effects. The inhibition of ERKs route with the inhibitor AG126 (sc3528) (Santa Cruz) was studied and the results indicate that this ERK inhibitor significantly blocks the decrease of catalase activity induced by VIP in A498 cells.

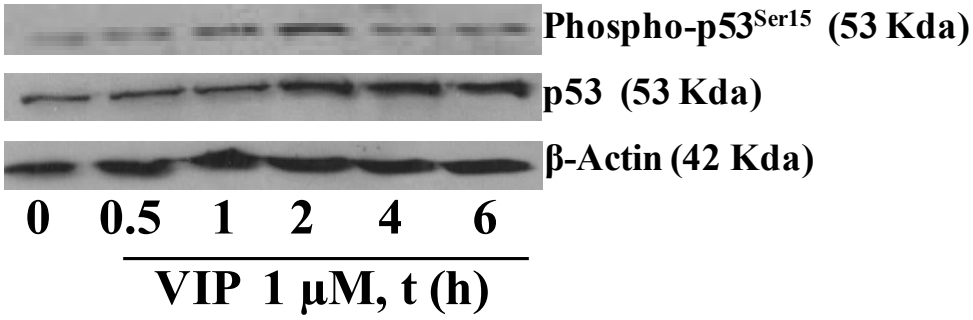

Annexe 4. VIP treatment of cells results in a significant increase of p53 expression after 2 h as compared to control conditions. The expression of p53 gradually diminishes but remains increased as compared to control after 4 and 6 h. The analysis of phospho-p53 (Ser15) expression shows a significant increase after 2 h of cell treatment with 1 µM in agreement with that shown for total protein. However, this increase of phosphorylation was not maintained at higher time periods.